

AdaSFormer: Adaptive Serialized Transformers for Monocular Semantic Scene Completion from Indoor Environments

Xuzhi Wang¹ Xinran Wu¹ Song Wang² Lingdong Kong^{3*} Ziping Zhao^{1*}

¹Tianjin Normal University ²Zhejiang University ³National University of Singapore

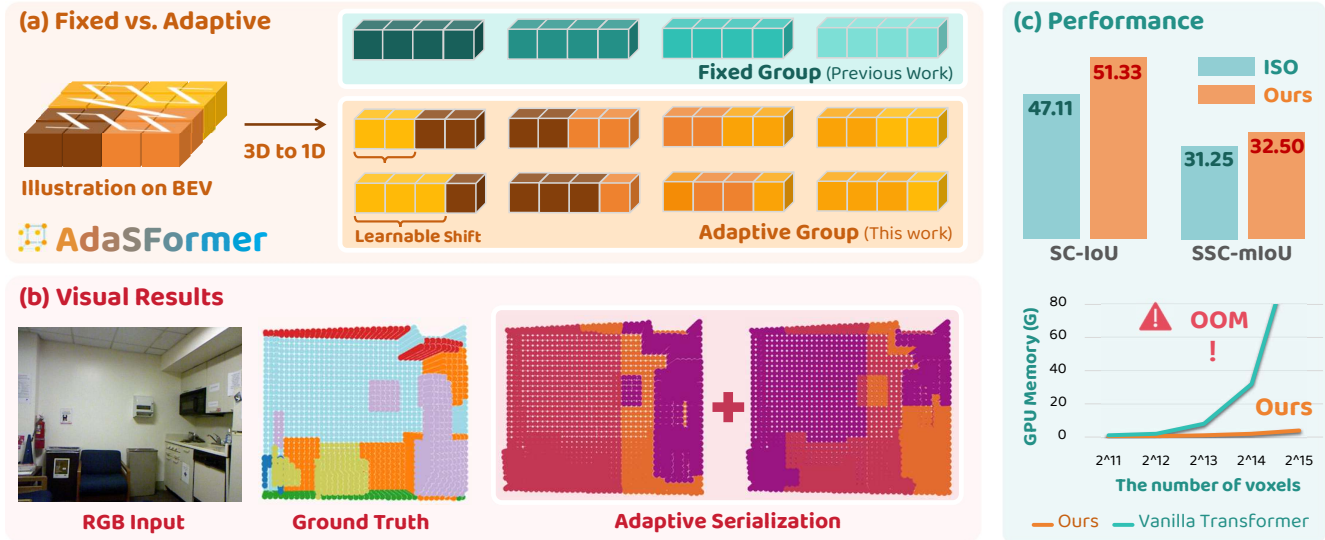


Figure 1. We introduce an **Adaptive Serialized Transformer (AdaSFormer)** to obtain a global receptive field for indoor 3D scene understanding, enabling the model to handle complex spatial layouts and severe occlusions. (1) Existing indoor approaches rely on convolution-based designs due to the high memory cost of Transformers, which limits their global modeling capacity. (2) Existing serialization-based methods assign a fixed receptive field to each patch. In contrast, our method employs a learnable shift mechanism that adaptively adjusts the receptive fields and coordinate features across layers, achieving more flexible and effective spatial representation. It is worth noting that we employ bird’s-eye view (BEV) representations to simplify the 3D voxels, enabling clearer and more intuitive visualization.

Abstract

Indoor monocular semantic scene completion (MSSC) is notably more challenging than its outdoor counterpart due to complex spatial layouts and severe occlusions. While transformers are well suited for modeling global dependencies, their high memory cost and difficulty in reconstructing fine-grained details have limited their use in indoor MSSC. To address these limitations, we introduce **AdaSFormer**, a serialized transformer framework tailored for indoor MSSC. Our model features **three** key designs: (1) an Adaptive Serialized Transformer with learnable shifts that dynamically adjust receptive fields; (2) a Center-Relative Positional Encoding that captures spatial information richness; and (3) a Convolution-Modulated Layer Normalization that bridges heterogeneous representations between convolutional and transformer features. Exten-

sive experiments on NYUv2 and Occ-ScanNet demonstrate that ASFormer achieves state-of-the-art performance. The code is publicly available at: <https://github.com/alanWXZ/AdaSFormer>.

1. Introduction

Monocular semantic scene completion (MSSC) has recently gained traction in the context of autonomous driving [3, 4, 76, 82, 101], as it enables holistic 3D understanding of complex outdoor environments from a single image [39, 68]. In contrast, indoor MSSC remains underexplored despite its fundamental importance to indoor scene perception, supporting applications in robot navigation, 3D reconstruction, and spatial understanding [5, 16, 29–31, 79, 80, 83, 84].

Indoor scenes differ substantially from outdoor settings [27, 28, 41, 42, 46, 81, 86]. Rather than featuring regular road layouts and open views, they contain intricate and multi-level spatial structures, including overlapping ceil-

*Corresponding authors.

ings, walls, and furniture, with frequent occlusions and high object density [6, 37, 75]. This complexity demands not only accurate local geometry but also strong global contextual reasoning to infer the geometry and semantics of occluded regions [74].

Most existing approaches heavily rely on convolutional architectures [64, 74, 90, 91]. However, their inherently limited receptive fields prevent them from modeling long-range dependencies effectively, while enlarging kernels in 3D incurs prohibitive cubic computational cost [9, 14]. Early convolutional layers propagate information solely within local neighborhoods, while deeper layers operate at reduced resolutions, leading to spatial information loss and degraded completion quality [17, 40, 52, 94].

Modeling long-range dependencies is therefore essential, making transformer architectures a natural choice [20, 50, 66]. Yet, applying transformers directly to dense 3D volumes remains computationally expensive and memory-intensive [22, 38, 39, 53, 77], especially for high-resolution indoor scenes [63, 91].

To address these challenges, we design *AdaFormer*, a hybrid framework that unifies convolutional and transformer modules, each serving complementary roles. The transformer operates on voxels containing valid features to capture global context, while the convolution focuses on local feature propagation and refinement. Our framework introduces **three** core designs: (1) *Adaptive Serialized Attention* (ASA), which employs learnable shifts to dynamically adjust receptive fields and coordinate features across layers; (2) *Center-Relative Positional Encoding* (CRPE), which encodes spatial information richness relative to the scene center; and (3) *Convolution-Modulated Layer Normalization* (CMLN), which harmonizes feature statistics between convolutional and transformer representations.

As illustrated in Fig. 2, given a single RGB image, a 2D encoder first extracts features and estimates depth, which are projected into 3D space via surface projection [45]. Within the 3D encoder, alternating transformer and convolutional modules jointly capture global context and complete 3D geometry, followed by a lightweight decoder that integrates multi-scale features to produce final semantic scene completion (SSC) results.

Our main contributions are summarized as follows:

- We propose *AdaFormer* to capture long-range dependencies while maintaining efficiency through complementary feature propagation, substantially reducing both memory footprint and computational overhead.
- We introduce three novel components, ¹*Adaptive Serialized Attention*, ²*Center-Relative Positional Encoding*, and ³*Convolution-Modulated Layer Normalization*, which collectively enhance receptive-field adaptability, spatial reasoning, and cross-module feature alignment.
- Extensive experiments on the NYUv2 and OccScanNet

datasets demonstrate that our approach achieves state-of-the-art performance against popular MSSC methods.

2. Related Work

Monocular Semantic Scene Completion (MSSC). Scene completion tasks predicts both voxel occupancy and semantic labels, providing holistic 3D scene understanding [36, 42, 70, 72, 73, 75]. The pioneering SSCNet [99] introduced indoor SSC using depth maps, later extended to RGB-D inputs [8, 33, 34, 45, 73] and outdoor perception [48, 49, 58, 78, 85, 88, 102]. Recent monocular SSC approaches [26, 32, 35, 39, 62, 69, 71, 93, 95, 97, 98, 101] further advance the task by relying solely on RGB images. For indoor scenarios, where lightweight deployment is critical, several representative works have emerged: MonoScene [4] bridges 2D-3D features via Line-of-Sight Projection; NDC-Scene [90] introduces normalized device coordinates to reduce depth ambiguity; ISO [91] enhances voxel learning with dual projection; and MonoMRN [74] adopts a masked recurrent refinement design. Most indoor MSSC methods are CNN-based, achieving efficiency but limited global reasoning. In contrast, our approach employs an adaptive serialized transformer to enlarge receptive fields while maintaining low computational cost.

Single-View 3D Reconstruction. Recovering 3D geometry from a single RGB image has long been studied for both objects and scenes [25, 47]. Early works reconstruct individual objects using explicit [1, 11, 15] or implicit [54, 55, 57] representations, while more recent efforts address full scene reconstruction [10, 44, 96]. Holistic reconstruction methods [12, 13, 43, 87, 92] recover the scene as a whole, often guided by depth estimation [4, 39, 91] and processed through encoder–decoder architectures. Compositional approaches [18, 19, 44, 100] reconstruct objects separately before assembling them via layout and pose estimation, as seen in DepR [96] and ComboVerse [10]. These reconstruction paradigms provide geometric priors and structural insights closely related to semantic scene completion.

Serialization-Based Approaches. The recent serialization-based transformers [7, 51, 67, 77] convert irregular 3D data into ordered sequences to enable efficient attention while preserving spatial locality. Representative works include OctFormer [67], which partitions point clouds via sorted octree keys; FlatFormer [51], which reduces padding through flattened window grouping; and PTv3 [77], which applies shuffle-based ordering with conditional positional encoding. Although designed mainly for 3D segmentation and detection, these methods demonstrate the efficiency of serialized attention for large-scale 3D modeling. Our work extends this idea to semantic scene completion through adaptive serialization with learnable shifts and center-relative positional encoding, improving long-range reasoning under sparse 3D layouts.

3. Methodology

In this section, we first provide an overview of our method. Next, we give a brief preliminary to voxel serialization (Sec. 3.1). Following this, we delve into the AdaSFormer network, including its three proposed key designs: Adaptive Serialized Attention (Sec. 3.2.1), Center-Relative Positional Encoding (Sec. 3.2.2), and the Conv-Modulated Layer Normalization (Sec. 3.2.3). Lastly, we introduce the loss function for model training (Sec. 3.2.4).

Problem Formulation. Given a single-view RGB image I_{RGB} that captures only a partial 3D scene, monocular semantic scene completion aims to predict the volumetric occupancy of the entire scene. Each voxel is assigned a semantic label C_i with $i \in [0, 1, \dots, N]$, where N is the number of object categories and C_0 denotes empty space.

Overall Network Architecture. From a single RGB image, 2D features are first extracted using EfficientNet [65], and the corresponding depth map is estimated using an off-the-shelf method [89]. Leveraging the estimated depth together with the camera’s intrinsic and extrinsic parameters, the 2D features are projected into 3D space. The resulting 3D representations are subsequently processed by a transformer-based encoder, consisting of a series of ASFormer blocks, followed by a decoder to produce the final Semantic Scene Completion (SSC) outputs. We refrain from employing a transformer-based architecture at the decoding stage, as the number of non-empty voxels increases significantly. In this setting, convolutional decoding offers higher efficiency than transformer-based decoding, effectively reducing computational overhead.

3.1. Preliminary of Voxel Serialization

In this section, we present preliminaries of serialization-based transformers. We introduce a voxel serialization-based method that enables 3D networks to capture a sufficiently large and high-resolution receptive field in the early stage while keeping memory consumption manageable, which is crucial for scene completion tasks.

Serialization. Serialization transforms irregular or high-dimensional spatial data into a structured sequential format suitable for attention-based modeling as shown in Fig. 3 (a). Specifically, given an input 3D voxel $X \in \mathbb{R}^{C \times D \times H \times W}$, we employ a space-filling curve (e.g., Z curve and Hilbert curve) to linearize the volumetric representation along a continuous path. This preserves the local spatial proximity of neighboring elements, allowing the attention mechanism to operate efficiently while maintaining spatial correlations. After serialization, the data is represented as a sequence of tokens $S = [s_1, s_2, \dots, s_N]$, where $N = D \times H \times W$.

Local Grouping. The core purpose of serialization is to enable more effective local grouping. Since the computational complexity of the attention mechanism grows quadratically with the input sequence length ($O(N^2)$), reasonable data

grouping is crucial for processing large-scale 3D data. Local grouping divides the serialized sequence into fixed-length groups, each containing G consecutive tokens. Attention is computed only within each group, which captures local dependencies while significantly reducing computational cost. Formally, the sequence is divided into $M = \lceil N/G \rceil$ groups, where $\lceil \cdot \rceil$ denotes the ceiling operation (i.e., rounding up), ensuring that all tokens are included:

$$S = [S_1, S_2, \dots, S_M], \quad S_i \in \mathbb{R}^{G \times C}. \quad (1)$$

Under this grouping, the computational complexity per group is $O(G^2)$, leading to a total complexity of $O(M \cdot G^2) = O(N \cdot G)$, which is much lower than the full attention complexity $O(N^2)$.

Compared with conventional window-attention [50] based grouping methods, serialization-based grouping for 3D data has the following advantages: 1) Avoids voxel padding overhead: 3D point clouds are often sparse, and in window-based grouping, the number of voxels in each window usually varies. Padding is required to unify the length, which wastes significant computational resources. In contrast, serialization-based grouping can evenly divide the non-empty voxels without additional padding, reducing redundant computation. 2) Larger effective receptive field: Window-based grouping includes empty voxels, limiting the local receptive field. Given the same number of tokens per group, serialization-based grouping removes empty voxels, allowing attention to operate over a wider range of valid spatial regions and capturing richer local contextual information.

3.2. AdaSFormer: Towards Efficient MSSC

Several stacked AdaSFormer blocks serve as the 3D network encoder, modeling global dependencies with moderate memory consumption.

3.2.1. Adaptive Serialized Attention (ASA)

Although the serialized transformer reduces GPU memory consumption by serializing patches, the obtained patches remain fixed once a specific serialization strategy is chosen. However, the grouping scheme also greatly affects the receptive field range. As illustrated in Figure 3, different starting points can significantly alter the receptive field: in some cases, the partitioned voxel range may fully cover a single object, thereby capturing its overall structure more effectively; in other cases, the voxel range may simultaneously include multiple objects and their spatial relationships. Such variations directly influence the model’s representational capacity at both local and global levels, as well as its ability to capture semantic correlations.

Therefore, obtaining an appropriate shift is crucial for serialized attention. However, existing serialized attention

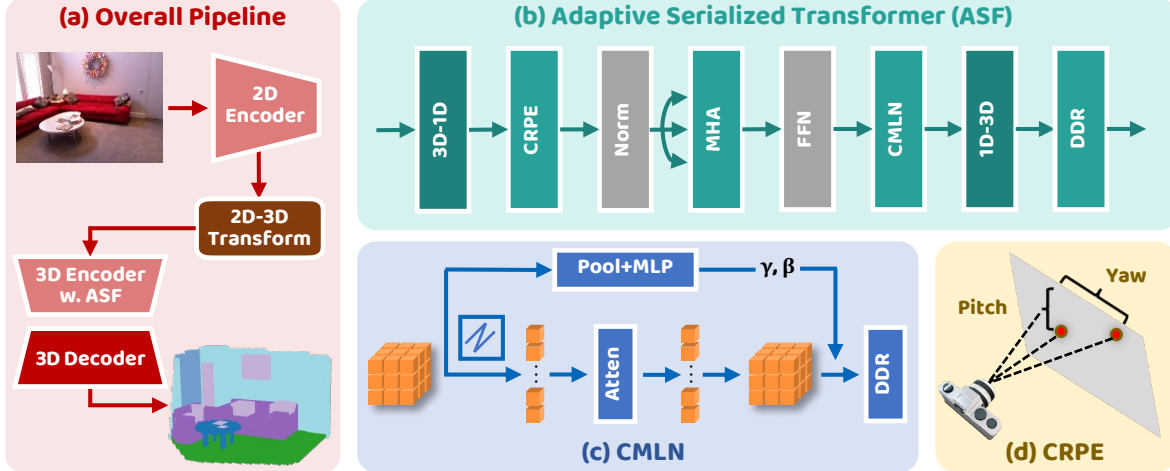


Figure 2. **AdaSFormer Framework.** (a) Overall network architecture: It mainly consists of a 2D encoder, a depth estimation network, a 2D-to-3D projection module, and a 3D network. (b) Adaptive Serialized Transformer (ASF): This is the core of our method. A set of ASF blocks forms the encoder of the 3D network. The 3D voxels are adaptively converted into 1D patches, which are then augmented with center-relative positional encoding. These patches are processed through standard self-attention and feed-forward layers. Through the proposed Convolution-Modulated Layer Normalization (CMLN), the heterogeneous features from the transformer and convolutional layers are bridged. The resulting features are then fed into a DDR block for scene completion. (c) Convolution-Modulated Layer Normalization (CMLN): Modulates features to integrate transformer and convolutional representations effectively. (d) Center-Relative Positional Encoding: Enhances the richness of input information by modeling the relative spatial relationships of patches.

methods do not consider the influence of patch shifts. For window-based attention mechanisms, although prior works such as the Swin Transformer [50] introduce the concept of window shifting, the shift size remains fixed and non-learnable. Moreover, since the Swin Transformer operates on 2D patches, its potential shift range is inherently constrained by the spatial window size. In contrast, serialized attention operates along a 1D voxel sequence, offering a broader and more flexible space for shift adjustment. This property makes it particularly suitable for incorporating learnable, data-driven shifts that can dynamically adapt the serialization starting point to better capture object structures and their spatial relationships.

Assuming a patch size of P , we introduce K learnable parameters to model the spatial offsets within each voxel group after serialization. Each parameter corresponds to a discrete shift value uniformly spaced by P/K ; that is, the k -th parameter represents a shift of $k \cdot (P/K)$. During training, these learnable offsets are optimized to capture the most informative spatial alignment of serialized voxels with respect to object boundaries or scene layouts, thereby improving the contextual consistency of the representation.

Straight-Through Gumbel-Softmax. By leveraging the differentiable relaxation provided by Gumbel-Softmax, the start point can be trained end-to-end. During training, we compute a straight-through estimator to allow gradient flow while maintaining discrete selections. Let \mathbf{l} denote the logits and τ the temperature. The soft Gumbel-Softmax output \mathbf{y}_{soft} and the hard one-hot output \mathbf{y}_{hard} are computed as:

$$\mathbf{y}_{\text{soft}} = \text{softmax}\left(\frac{\mathbf{l} + \mathbf{g}}{\tau}\right), \quad \mathbf{g} \sim \text{Gumbel}(0, 1), \quad (2)$$

$$\mathbf{y}_{\text{hard}} = \text{one_hot}\left(\arg \max_i \mathbf{y}_{\text{soft}, i}\right). \quad (3)$$

The straight-through (ST) Gumbel-Softmax output is then given by:

$$\mathbf{y}_{\text{ST}} = \mathbf{y}_{\text{hard}} + \mathbf{y}_{\text{soft}} - \mathbf{y}_{\text{soft}} \cdot \text{detach}(). \quad (4)$$

In this formulation, the forward pass uses the discrete \mathbf{y}_{hard} , while the gradient during backpropagation flows through \mathbf{y}_{soft} , enabling differentiable learning with discrete selections.

Temperature Annealing Strategy. We design a temperature annealing strategy to allow the network to better learn discrete selections. Specifically, the temperature τ in the Gumbel-Softmax is gradually decreased during training to control the discreteness of the sampling. At epoch t , τ is updated as:

$$\tau_t = \max\left(\tau_{\min}, \tau_{\text{init}} \cdot \exp(-\alpha t)\right), \quad (5)$$

where τ_{init} is the initial temperature, τ_{\min} is the minimum temperature, and α is the annealing rate.

3.2.2. Center-Relative Positional Encoding (CRPE)

Since our algorithm adopts a hybrid architecture of CNN and Transformer, where the CNN effectively captures local positional information, the model has a reduced reliance

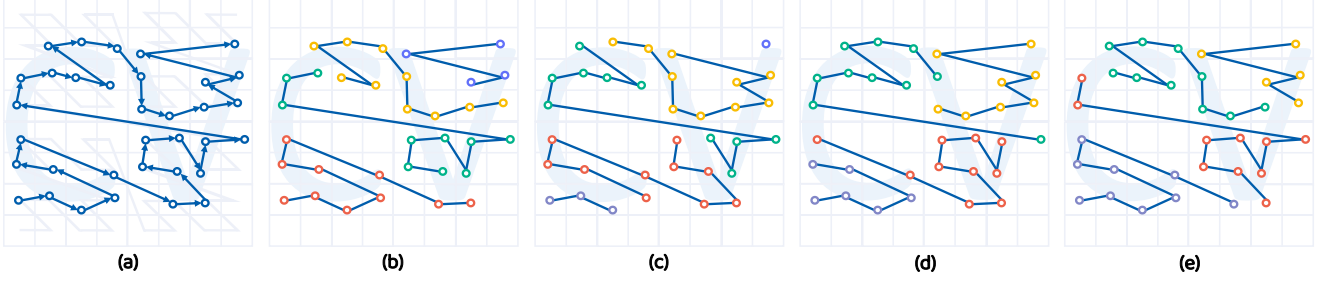


Figure 3. (a) illustrates the Z-order serialization of a 2D image, as well as that of a sparse 2D image, where the letters “C” and “V” in the figure indicate the locations of objects in the spatial domain. (b)-(e) illustration of Z-order serialization with shifts of 0, 3, 6, and 9 (from left to right). Different shift settings significantly affect the coverage and overlap between adjacent patches, especially for large patch sizes.

on traditional positional encoding. Inspired by work [2], which demonstrates that the spatial distribution of input information in 3D space has a significant impact on SSC performance. Based on this observation, we design a positional encoding scheme to model this information richness. Specifically, we compute the yaw and pitch angles between each point and the scene center to describe their relative spatial relationships. This encoding enables the model to perceive the spatial relations between different regions and the scene center, allowing it to identify areas that are more likely to contain key structural or semantic information, and thereby allocate attention and feature weights more effectively.

We compute the scene center \mathbf{c} as the mean coordinate of all occupied voxels:

$$\mathbf{c} = \frac{\sum_{i=1}^M \mathbf{p}_i \cdot \mathbf{1}(v_i > 0)}{\sum_{i=1}^M \mathbf{1}(v_i > 0)}, \quad (6)$$

where $\mathbf{p}_i = (x_i, y_i, z_i)$ denotes the center coordinate of the i -th voxel, v_i is its occupancy value, $\mathbf{1}(v_i > 0)$ is an indicator function that equals 1 if the voxel is occupied and 0 otherwise, and \mathbf{c} represents the mean coordinate of all occupied voxels, *i.e.*, the scene center.

The yaw angle (horizontal rotation around the vertical axis) for each voxel and for the grid center is defined as:

$$\theta^i = \text{atan2}(d_x^i, d_y^i), \quad (7)$$

$$\theta^c = \text{atan2}(d_x^c, d_y^c), \quad (8)$$

where d_x^i and d_y^i are the x and y components of the vector \mathbf{d}^i . The yaw difference between voxel i and the center is then given by:

$$\Delta\theta^i = \theta^i - \theta^c. \quad (9)$$

Similarly, the pitch angle (vertical inclination) for each voxel and for the grid center are defined as:

$$\phi^i = \text{atan2}\left(d_z^i, \sqrt{(d_x^i)^2 + (d_y^i)^2}\right), \quad (10)$$

$$\phi^c = \text{atan2}\left(d_z^c, \sqrt{(d_x^c)^2 + (d_y^c)^2}\right), \quad (11)$$

and the pitch difference is computed as:

$$\Delta\phi^i = \phi^i - \phi^c. \quad (12)$$

After obtaining $\Delta\phi$ and $\Delta\theta$, we concatenate them into a single feature vector, which is then processed by a multi-layer perceptron (MLP). The resulting output is used as a bias added to the serialized attention.

3.2.3. Convolution-Modulated Layer Norm (CMLN)

Since transformers and convolutional networks extract fundamentally different types of features, directly interleaving these modules can cause learning difficulties and limit performance gains. To address this, we propose Conv-Modulated Layer Normalization motivated by [56]. Specifically, after voxel features X_{voxel} are serialized and processed by Serialized Attention, they are modulated through Conv-Modulated Layer Normalization before being fed into the DDR module, a lightweight component designed for semantic scene completion (SSC) refinement.

The Conv-Modulated Layer Normalization can be defined as follows:

$$\text{CMLN}(h_i | X_{\text{voxel}}) = \gamma(X_{\text{voxel}}) \odot \frac{h_i - \mu_i}{\sigma_i} + \beta(X_{\text{voxel}}), \quad (13)$$

where h_i denotes the features to be normalized, μ_i and σ_i are the mean and standard deviation computed over the feature dimension, and $\gamma(X_{\text{voxel}})$, $\beta(X_{\text{voxel}})$ are functions (*e.g.*, small MLPs) that produce the normalization parameters from the voxel features. This design allows the network to adaptively modulate feature statistics based on the input context.

After the Convolution-Modulated Layer Normalization, the features are fed into the DDR block [33], a lightweight 3D convolutional module designed for semantic scene completion. The Adaptive Serialized Attention captures global

Table 1. **Comparisons among state-of-the-art MSSC methods** on the NYUv2 dataset [63]. The symbol † denotes the results presented by [4]. The **Best** and **2nd Best** scores from each metric are highlighted in **Orange** and **Teal**, respectively.

Method	Venue	SC IoU (%)	Ceiling	Floor	Wall	window	chair	bed	sofa	table	tv	furniture	objects	SSC mIoU (%)
LMSCNet† [60]	3DV’20	33.93	4.49	88.41	4.63	0.25	3.94	32.03	15.44	6.57	0.02	14.51	4.39	15.88
AICNet† [34]	CVPR’20	30.03	7.58	82.97	9.15	0.05	6.93	35.87	22.92	11.11	0.71	15.90	6.45	18.15
3DSketch† [8]	CVPR’20	38.64	8.53	90.45	9.94	5.67	10.64	42.29	29.21	13.88	9.38	23.83	8.19	22.91
MonoScene [4]	CVPR’22	42.51	8.89	93.50	12.06	12.57	13.72	48.19	36.11	15.13	15.22	27.96	12.94	26.94
NDC-Scene [90]	ICCV’23	44.17	12.02	93.51	13.11	13.77	15.83	49.57	39.87	17.17	24.57	31.00	14.96	29.03
ISO [91]	ECCV’24	47.11	14.21	93.47	15.89	15.14	18.35	50.01	40.82	18.25	25.90	34.08	17.67	31.25
MonoMRN [74]	ICCV’25	53.16	26.80	92.02	19.39	18.50	17.66	44.60	31.02	19.60	17.22	32.90	18.31	30.73
GenFuSE [61]	arXiv’25	46.30	9.80	92.80	13.80	13.70	17.60	48.60	39.70	17.60	24.70	33.40	17.20	29.90
AdaSFormer	Ours	51.33	16.18	92.72	16.96	14.10	23.93	53.89	44.52	16.65	23.85	35.97	18.67	32.50

contextual dependencies, while the convolution propagates information to spatially neighboring regions, effectively enhancing local geometric representations. Moreover, by incorporating convolutional operations, the Transformer avoids computing attention over all voxels, thereby reducing computational overhead.

3.2.4. Loss Function

Our method is trained end-to-end from scratch by applying cross-entropy loss, geometric affinity loss, and semantic affinity loss [4]:

$$\mathcal{L}_{\text{total}} = \mathcal{L}_{\text{ce}} + \mathcal{L}_{\text{scal}}^{\text{sem}} + \mathcal{L}_{\text{scal}}^{\text{geo}}, \quad (14)$$

where $\mathcal{L}_{\text{scal}}$ denotes the Scene-Class Affinity Loss proposed by MonoScene [4].

4. Experiments

We conduct experiments on the widely used NYUv2 dataset [63] as well as the large-scale indoor dataset Occ-ScanNet [91]. The proposed approach is compared against state-of-the-art methods, and both experimental results and ablation studies are thoroughly analyzed. In addition, we present qualitative visualizations to further illustrate the effectiveness of our proposed method.

4.1. Experimental Setup

Datasets. The NYUv2 dataset [63] consists of 1,449 depth images captured with a Kinect sensor across diverse indoor scenes, split into 795 for training and 654 for testing. Following SSCNet [64], we employ the 3D voxel annotations provided by [59] and adopt the category mappings defined in [21]. The Occ-ScanNet dataset [91] serves as a large-scale benchmark for indoor 3D semantic scene completion. It contains 45,755 training frames and 19,764 validation frames, with scenes voxelized into grids of $60 \times 60 \times 36$.

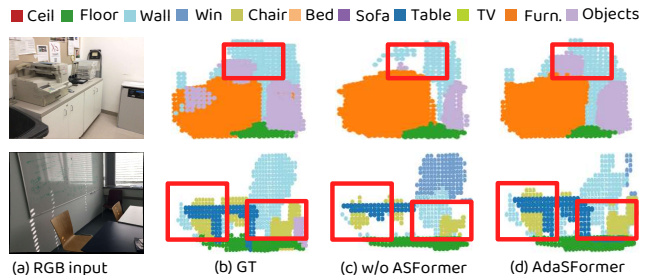


Figure 4. Visualization of the ablation results on the Occ-ScanNet dataset [91]. Introducing AdaSFormer significantly improves the model’s capability to capture spatial and semantic relationships, leading to more complete and coherent object completion.

Both NYUv2 and Occ-ScanNet are annotated with the same 12 semantic classes: one for empty (free space) and eleven for typical indoor categories, including *ceiling*, *floor*, *wall*, *window*, *chair*, *bed*, *sofa*, *table*, *television*, *furniture*, and *miscellaneous objects*.

Evaluation Metrics. For fair comparison, we follow the evaluation protocol of SSCNet [64]. In semantic scene completion (SSC), performance is measured using the intersection over union (IoU) between predicted and ground-truth voxel labels for each semantic class, and the overall accuracy is reported as the mean IoU (mIoU) across all classes. For scene completion (SC), voxels are classified into empty or occupied, and performance is evaluated using IoU.

Implementation details. We implement our approach using the PyTorch framework. The model is optimized with stochastic gradient descent (SGD), starting from an initial learning rate of 0.1 for NYUv2 and 0.003 for Occ-ScanNet, which is adjusted according to the polynomial learning rate policy. We train the network for 100 epochs. The output 3D feature maps have dimensions of $60 \times 36 \times 60$ for NYUv2 and $60 \times 60 \times 36$ for Occ-ScanNet. All experiments are conducted on an NVIDIA A100 GPU.

Table 2. **Comparisons among state-of-the-art MSSC methods** on the **Occ-ScanNet** dataset [91]. The symbol † denotes the results presented by [4]. The **Best** and **2nd Best** scores from each metric are highlighted in **Orange** and **Teal**, respectively. Symbol * denotes the results obtained using their official code trained on the Occ-ScanNet dataset.

Method	Venue	IoU (%)	ceiling	floor	wall	window	chair	bed	sofa	table	tv	furniture	objects	mIoU (%)
TPVFormer [23]	CVPR'23	33.39	6.96	32.97	14.41	9.10	24.01	41.49	45.44	28.61	10.66	35.37	25.31	24.94
GaussianFormer [24]	ECCV'24	40.91	20.70	42.00	23.40	17.40	27.0	44.30	44.80	32.70	15.30	36.70	25.00	29.93
MonoScene [4]	CVPR'22	41.60	15.17	44.71	22.41	12.55	26.11	27.03	35.91	28.32	6.57	32.16	19.84	24.62
ISO [91]	ECCV'24	42.16	19.88	41.88	22.37	16.98	29.09	42.43	42.00	29.60	10.62	36.36	24.61	28.71
SurroundOCC [76]	ICCV'23	42.52	18.90	49.30	24.80	18.00	26.80	42.00	44.10	32.90	18.60	36.80	26.90	30.83
AdaSFormer	Ours	54.63	37.66	57.34	40.51	29.49	43.29	60.41	63.08	47.05	29.63	54.08	36.15	45.33

Table 3. Ablation study on the core components in the proposed framework.

Method	SC-IoU (%) †	SSC-mIoU (%) †
Baseline	47.43	28.68
+ ASA	50.11 (+2.68)	30.98 (+2.30)
+ CRPE	50.71 (+0.60)	31.66 (+0.68)
+ CMF	51.33 (+0.62)	32.50 (+0.84)

Table 4. Ablation study on different Adaptive Serialized Attention configurations.

Method	SC-IoU (%) †	SSC-mIoU (%) †
Baseline	47.43	28.68
+ VanillaShift	49.76 (+2.33)	30.61 (+1.93)
+ GumbelShift	50.87 (+1.11)	31.96 (+1.35)
+ AnnealedShift	51.33 (+0.46)	32.50 (+0.54)

Table 5. Ablation study on the Center-Relative Positional Encoding setups.

Method	SC-IoU (%) †	SSC-mIoU (%) †
w/o CRPE	50.85	32.06
w/o PVM	50.89	32.11
w/o RYP	50.96	32.23
with CRPE	51.33	32.50

4.2. Comparisons with State of the Arts

Quantitative Comparisons. The results of the quantitative comparisons are presented in Tables 1 and 2. It can be seen that our method achieves the best performance on the SSC task. On the NYU v2 dataset, our approach surpasses the current state-of-the-art method, ISO, by 1.25 mIoU, achieving a total of 32.50 mIoU. Similarly, on the OCC-ScanNet dataset, our method outperforms the best existing method, ISO, by 14.50 mIoU, reaching 45.33 mIoU.

Qualitative Assessments. The Fig. 5 presents the visual comparison results of our method, the Baseline, and the ISO method on the NYU v2 dataset. It can be observed that our approach achieves superior performance in the Semantic Scene Completion (SSC) task. Benefiting from the proposed AdaSFormer model, our method is able to obtain a sufficiently large receptive field in the early stages of the network, enabling more effective capture of global spatial structures and enhancing the completeness and semantic consistency of the overall reconstruction. As shown in Fig. 5, it is evident that the increased receptive field facilitates more accurate scene completion and enhances the ability to distinguish between different objects in the scene.

4.3. Ablation Study

We present exhaustive ablation experiments on the NYUv2 dataset [63] to evaluate the effectiveness of our method from several perspectives, focusing on key components such as Adaptive Serialized Attention (ASA) and Center-Relative Positional Encoding (CRPE). Due to space constraints, more details and visualizations are provided in the

supplementary material.

The Effectiveness of Core Components. Firstly, we conduct a systematic ablation study on the core components of proposed AdaSFormer, including the Adaptive Serialized Transformer (ASA), Center-Relative Positional Encoding (CRPE), and Conv-Modulated Former Block (CMF). By removing each module individually, we quantitatively analyze the contribution of each component to the overall performance, thereby gaining a deeper understanding of the rationale and advantages behind our design. The experimental results are presented in the Tab. 3, where ASA, CRPE, and CMF denote the corresponding modules, and Baseline refers to the network with all three modules removed, retaining only the remaining convolutional structure. By incorporating ASA, we can observe an improvement over the baseline of 2.68 in IoU and 2.30 in mIoU. Adding CRPE further increases the performance by 0.60 in IoU and 0.68 in mIoU, while the inclusion of CMF brings an additional improvement of 0.62 in IoU and 0.84 in mIoU.

Furthermore, we present visualization results comparing the model with and without the AdaSFormer module to more intuitively demonstrate its effectiveness. As shown in Fig. 4, incorporating the AdaSFormer module significantly enhances the model’s spatial perception capability, enabling it to better capture the spatial layout and semantic relationships among objects in the scene. Consequently, the model can more effectively recover occluded or missing structures in complex environments.

Design Choices of Adaptive Serialized Attention. We also perform ablation experiments on several key design choices of the Adaptive Serialized Attention, including

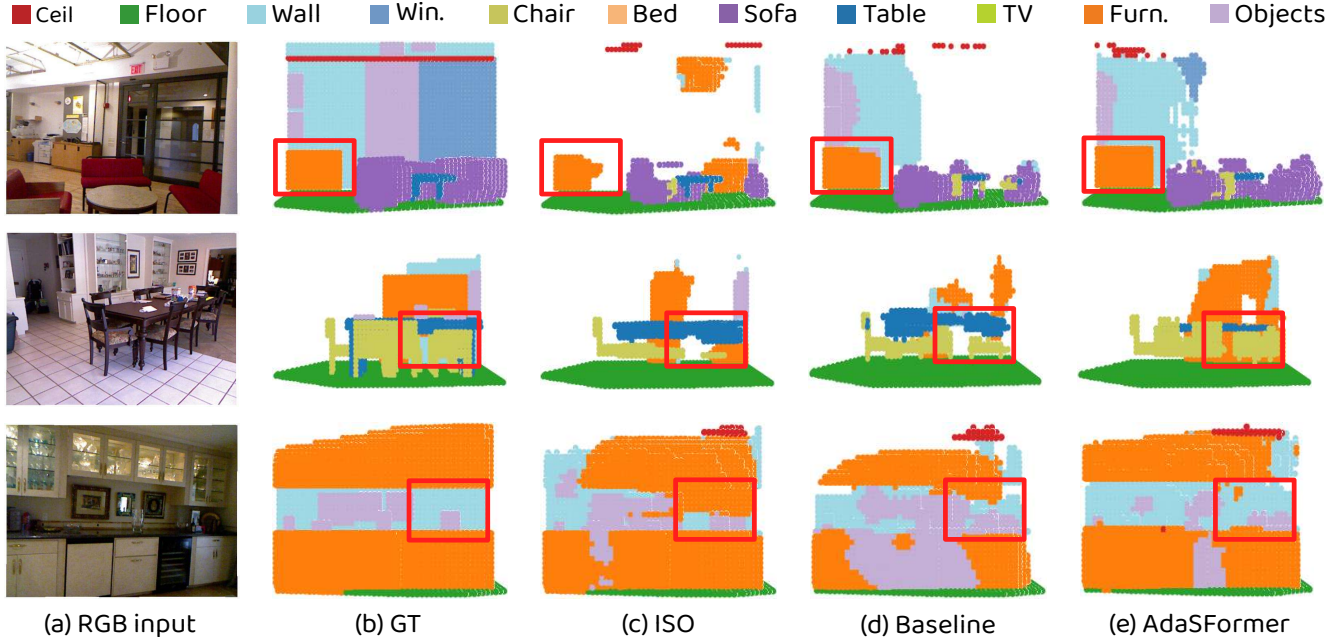


Figure 5. **Qualitative Comparisons** of semantic scene completion results on the NYUv2 testset [63] with different methods. Figures from left to right: (a) The single RGB input; (b) The ground truth; (c) ISO [91]; (d) Baseline; and (e) Our proposed method.

Table 6. Latency (in ms) study on each component.

Method	ISO [91]	AdaSFormer	w/o ADA	w/o CRPE	w/o CMLN
Latency	535.2	178.9	156.0	177.4	174.3

Vanilla Serialized Transformer, Gumbel-Softmax learning, and the temperature annealing strategy. As illustrated in Tab. 4, ‘Baseline’ represents the model without the Adaptive Serialized Transformer block. ‘VanillaShift’ uses `torch.nn.Parameter` to directly learn n discrete shifts for n serialized intervals. ‘GumbelShift’ adopts the straight-through Gumbel-Softmax for discrete shift learning. In addition, the temperature annealing strategy is introduced to progressively adjust the Gumbel-Softmax during training. We observe that introducing Gumbel-Softmax improves the SSC performance by 1.35 mIoU, while further applying temperature annealing brings an additional 0.54 mIoU gain, demonstrating the effectiveness of these strategies in stabilizing optimization and enhancing adaptive shift learning.

Design Choices of Center-Relative Positional Encoding. We further validate two key design choices of the center-relative positional encoding, including projected voxel mean (PVM) and the effectiveness of relative yaw and pitch positional encoding (RPY). As shown in Tab. 5, for NYU v2, we observe that replacing the projected voxel mean (PVM) with the scene physical center at position [30, 18, 30] results in a drop of 0.39 mIoU, while removing the relative yaw and pitch positional encoding (RYP) leads to a decrease of 0.27 mIoU.

Effect of Key Components on Computational Efficiency.

In the end, we evaluate the computational efficiency of each component, including Adaptive Serialized Attention (ASA), Center-Relative Positional Encoding (CRPE), and Convolution-Modulated Layer Normalization (CMLN). As shown in Tab. 6, AdaSFormer achieves a latency of 178.9 ms, which is significantly lower than ISO [91] (535.2 ms), demonstrating the efficiency of the proposed architecture. Removing individual modules leads to only marginal latency variations (156.0 ms without ASA, 177.4 ms without CRPE, and 174.3 ms without CMLN), indicating that all components are lightweight. ASA introduces a small overhead of 22.9 ms while contributing substantially to performance improvement, confirming the balance between efficiency and accuracy.

5. Conclusion

In this paper, we propose a novel Adaptive Serialized Transformer (AdaSFormer) framework for indoor monocular semantic scene completion, which incorporates three key designs: 1) an Adaptive Serialized Attention that enables a larger, high-resolution, and adaptive receptive field; 2) a Center-Relative Positional Encoding that captures the spatial information richness to better represent scene structure; and 3) a Conv-Modulated Layer Normalization that facilitates the integration of Transformer and convolutional architectures, leading to a lightweight yet effective design. Extensive experiments on NYUv2 and Occ-ScanNet demonstrate the superiority of our method, achieving state-of-the-art performance across multiple datasets.

Acknowledgments

This work was supported by the National Natural Science Foundation of China under Grant No. 62071330.

The authors would like to sincerely thank the Program Chairs, Area Chairs, and Reviewers for the time and effort devoted during the review process.

References

- [1] Panos Achlioptas, Olga Diamanti, Ioannis Mitliagkas, and Leonidas Guibas. Learning representations and generative models for 3D point clouds. In *International Conference on Machine Learning*, pages 40–49. PMLR, 2018.
- [2] Jongseong Bae, Junwoo Ha, and Ha Young Kim. Three cars approaching within 100M! enhancing distant geometry by tri-axis voxel scanning for camera-based semantic scene completion. In *IEEE/CVF Conference on Computer Vision and Pattern Recognition*, pages 11939–11948, 2025.
- [3] Hengwei Bian et al. DynamicCity: Large-scale 4D occupancy generation from dynamic scenes. In *International Conference on Learning Representations*, 2025.
- [4] Anh-Quan Cao and Raoul De Charette. MonoScene: Monocular 3D semantic scene completion. In *IEEE/CVF Conference on Computer Vision and Pattern Recognition*, pages 3991–4001, 2022.
- [5] Runnan Chen et al. CLIP2Scene: Towards label-efficient 3D scene understanding by CLIP. In *IEEE/CVF Conference on Computer Vision and Pattern Recognition*, pages 7020–7030, 2023.
- [6] Runnan Chen et al. Towards label-free scene understanding by vision foundation models. In *Advances in Neural Information Processing Systems*, pages 75896–75910, 2023.
- [7] Wanli Chen, Xinge Zhu, Guojin Chen, and Bei Yu. Efficient point cloud analysis using Hilbert curve. In *European Conference on Computer Vision*, pages 730–747. Springer, 2022.
- [8] Xiaokang Chen, Kwan-Yee Lin, Chen Qian, Gang Zeng, and Hongsheng Li. 3D sketch-aware semantic scene completion via semi-supervised structure prior. In *IEEE/CVF Conference on Computer Vision and Pattern Recognition*, pages 4193–4202, 2020.
- [9] Yukang Chen, Jianhui Liu, Xiangyu Zhang, Xiaojuan Qi, and Jiaya Jia. LargeKernel3D: Scaling up kernels in 3D sparse CNNs. In *IEEE/CVF Conference on Computer Vision and Pattern Recognition*, pages 13488–13498, 2023.
- [10] Yongwei Chen, Tengfei Wang, Tong Wu, Xingang Pan, Kui Jia, and Ziwei Liu. ComboVerse: Compositional 3D assets creation using spatially-aware diffusion guidance. In *European Conference on Computer Vision*, pages 128–146. Springer, 2024.
- [11] Christopher B Choy, Danfei Xu, JunYoung Gwak, Kevin Chen, and Silvio Savarese. 3D-R2N2: A unified approach for single and multi-view 3D object reconstruction. In *European Conference on Computer Vision*, pages 628–644. Springer, 2016.
- [12] Tao Chu, Pan Zhang, Qiong Liu, and Jiaqi Wang. BUOL: A bottom-up framework with occupancy-aware lifting for panoptic 3D scene reconstruction from a single image. In *IEEE/CVF Conference on Computer Vision and Pattern Recognition*, pages 4937–4946, 2023.
- [13] Manuel Dahnert, Ji Hou, Matthias Nießner, and Angela Dai. Panoptic 3D scene reconstruction from a single rgb image. *Advances in Neural Information Processing Systems*, 34:8282–8293, 2021.
- [14] Xiaohan Ding, Xiangyu Zhang, Jungong Han, and Guiguang Ding. Scaling up your kernels to 31x31: Revisiting large kernel design in cnns. In *IEEE/CVF Conference on Computer Vision and Pattern Recognition*, pages 11963–11975, 2022.
- [15] Haoqiang Fan, Hao Su, and Leonidas J Guibas. A point set generation network for 3D object reconstruction from a single image. In *IEEE/CVF Conference on Computer Vision and Pattern Recognition*, pages 605–613, 2017.
- [16] Sicheng Feng, Song Wang, Shuyi Ouyang, et al. Can MLLMs guide me home? a benchmark study on fine-grained visual reasoning from transit maps. *arXiv preprint arXiv:2505.18675*, 2025.
- [17] Tuo Feng, Wenguan Wang, Fan Ma, and Yi Yang. LSK3DNet: Towards effective and efficient 3D perception with large sparse kernels. In *IEEE/CVF Conference on Computer Vision and Pattern Recognition*, pages 14916–14927, 2024.
- [18] Daoyi Gao, Dávid Rozenberszki, Stefan Leutenegger, and Angela Dai. Diffcad: Weakly-supervised probabilistic cad model retrieval and alignment from an RGB image. *ACM Transactions on Graphics*, 43(4):1–15, 2024.
- [19] Can Gümelí, Angela Dai, and Matthias Nießner. Roca: Robust CAD model retrieval and alignment from a single image. In *IEEE/CVF Conference on Computer Vision and Pattern Recognition*, pages 4022–4031, 2022.
- [20] Kai Han, Yunhe Wang, Hanqing Chen, Xinghao Chen, Jianyuan Guo, Zhenhua Liu, Yehui Tang, An Xiao, Chunjing Xu, Yixing Xu, et al. A survey on vision transformer. *IEEE Transactions on Pattern Analysis and Machine Intelligence*, 45(1):87–110, 2022.
- [21] Ankur Handa, Viorica Patraucean, Vijay Badrinarayanan, Simon Stent, and Roberto Cipolla. SceneNet: Understanding real world indoor scenes with synthetic data. In *IEEE/CVF Conference on Computer Vision and Pattern Recognition*, pages 4077–4085, 2016.
- [22] Chenhang He, Ruihuang Li, Shuai Li, and Lei Zhang. Voxel set transformer: A set-to-set approach to 3d object detection from point clouds. In *IEEE/CVF Conference on Computer Vision and Pattern Recognition*, pages 8417–8427, 2022.
- [23] Yuanhui Huang, Wenzhao Zheng, Yunpeng Zhang, Jie Zhou, and Jiwen Lu. Tri-perspective view for vision-based 3D semantic occupancy prediction. In *IEEE/CVF Conference on Computer Vision and Pattern Recognition*, pages 9223–9232, 2023.
- [24] Yuanhui Huang, Wenzhao Zheng, Yunpeng Zhang, Jie Zhou, and Jiwen Lu. GaussianFormer: Scene as gaussians for vision-based 3D semantic occupancy prediction. In *European Conference on Computer Vision*, pages 376–393. Springer, 2024.

- [25] Maximilian Jaritz, Tuan-Hung Vu, Raoul de Charette, Emilie Wirbel, and Patrick Pérez. xMUDA: Cross-modal unsupervised domain adaptation for 3D semantic segmentation. In *IEEE/CVF Conference on Computer Vision and Pattern Recognition*, pages 12605–12614, 2020.
- [26] Haoyi Jiang, Tianheng Cheng, Naiyu Gao, Haoyang Zhang, Tianwei Lin, Wenyu Liu, and Xinggong Wang. Symphonize 3D semantic scene completion with contextual instance queries. In *IEEE/CVF Conference on Computer Vision and Pattern Recognition*, pages 20258–20267, 2024.
- [27] Lingdong Kong, Youquan Liu, Xin Li, Runnan Chen, Wenwei Zhang, Jiawei Ren, Liang Pan, Kai Chen, and Ziwei Liu. Robo3D: Towards robust and reliable 3D perception against corruptions. In *IEEE/CVF International Conference on Computer Vision*, pages 19994–20006, 2023.
- [28] Lingdong Kong, Jiawei Ren, Liang Pan, and Ziwei Liu. LaserMix for semi-supervised LiDAR semantic segmentation. In *IEEE/CVF Conference on Computer Vision and Pattern Recognition*, pages 21705–21715, 2023.
- [29] Lingdong Kong, Xiang Xu, Jiawei Ren, et al. Multi-modal data-efficient 3D scene understanding for autonomous driving. *IEEE Transactions on Pattern Analysis and Machine Intelligence*, 47(5):3748–3765, 2025.
- [30] Lingdong Kong, Wesley Yang, Jianbiao Mei, Youquan Liu, Ao Liang, Dekai Zhu, Dongyue Lu, Wei Yin, Xiaotao Hu, Mingkai Jia, Junyuan Deng, Kaiwen Zhang, Yang Wu, Tianyi Yan, Shenyuan Gao, Song Wang, Linfeng Li, Liang Pan, Yong Liu, Jianke Zhu, Wei Tsang Ooi, Steven C. H. Hoi, and Ziwei Liu. 3D and 4D world modeling: A survey. *arXiv preprint arXiv:2509.07996*, 2025.
- [31] Lingdong Kong, Xiang Xu, Youquan Liu, Jun Cen, Runnan Chen, Wenwei Zhang, Liang Pan, Kai Chen, and Ziwei Liu. LargeAD: Large-scale cross-sensor data pretraining for autonomous driving. *IEEE Transactions on Pattern Analysis and Machine Intelligence*, 48(2):1291–1308, 2026.
- [32] Bohan Li, Jiajun Deng, Wenyao Zhang, Zhuji Liang, Dalong Du, Xin Jin, and Wenjun Zeng. Hierarchical temporal context learning for camera-based semantic scene completion. In *European Conference on Computer Vision*, pages 131–148. Springer, 2024.
- [33] Jie Li, Yu Liu, Dong Gong, Qinfeng Shi, Xia Yuan, and Chunxia Zhao. RGBD based dimensional decomposition residual network for 3D semantic scene completion. In *IEEE/CVF Conference on Computer Vision and Pattern Recognition*, pages 7693–7702, 2019.
- [34] Jie Li, Kai Han, Peng Wang, Yu Liu, and Xia Yuan. Anisotropic convolutional networks for 3D semantic scene completion. In *IEEE/CVF Conference on Computer Vision and Pattern Recognition*, pages 3351–3359, 2020.
- [35] Jinke Li, Xiao He, Chonghua Zhou, Xiaoqiang Cheng, Yang Wen, and Dan Zhang. ViewFormer: Exploring spatiotemporal modeling for multi-view 3D occupancy perception via view-guided transformers. In *European Conference on Computer Vision*, pages 90–106. Springer, 2024.
- [36] Rong Li, Yuhao Dong, Tianshuai Hu, Ao Liang, et al. 3EED: Ground everything everywhere in 3D. *arXiv preprint arXiv:2511.01755*, 2025.
- [37] Rong Li et al. SeeGround: See and ground for zero-shot open-vocabulary 3D visual grounding. In *IEEE/CVF Conference on Computer Vision and Pattern Recognition*, pages 3707–3717, 2025.
- [38] Yanwei Li, Yilun Chen, Xiaojuan Qi, Zeming Li, Jian Sun, and Jiaya Jia. Unifying voxel-based representation with transformer for 3d object detection. *Advances in Neural Information Processing Systems*, 35:18442–18455, 2022.
- [39] Yiming Li, Zhiding Yu, Christopher Choy, Chaowei Xiao, Jose M Alvarez, Sanja Fidler, Chen Feng, and Anima Anandkumar. VoxFormer: Sparse voxel transformer for camera-based 3D semantic scene completion. In *IEEE/CVF Conference on Computer Vision and Pattern Recognition*, pages 9087–9098, 2023.
- [40] Ye Li, Lingdong Kong, Hanjiang Hu, Xiaohao Xu, and Xiaonan Huang. Is your LiDAR placement optimized for 3D scene understanding? In *Advances in Neural Information Processing Systems*, pages 34980–35017, 2024.
- [41] Ao Liang et al. LiDARcrafter: Dynamic 4D world modeling from LiDAR sequences. *arXiv preprint arXiv:2508.03692*, 2025.
- [42] Ao Liang et al. Perspective-invariant 3D object detection. In *IEEE/CVF International Conference on Computer Vision*, pages 27725–27738, 2025.
- [43] Haolin Liu, Yujian Zheng, Guanying Chen, Shuguang Cui, and Xiaoguang Han. Towards high-fidelity single-view holistic reconstruction of indoor scenes. In *European Conference on Computer Vision*, pages 429–446. Springer, 2022.
- [44] Ruoshi Liu, Rundui Wu, Basile Van Hoorick, Pavel Tokmakov, Sergey Zakharov, and Carl Vondrick. Zero-1-to-3: Zero-shot one image to 3D object. In *IEEE/CVF International Conference on Computer Vision*, pages 9298–9309, 2023.
- [45] Shice Liu, Yu Hu, Yiming Zeng, Qiankun Tang, Beibei Jin, Yinhe Han, and Xiaowei Li. See and think: Disentangling semantic scene completion. In *Advances in Neural Information Processing Systems*, pages 261–272, 2018.
- [46] Youquan Liu et al. Segment any point cloud sequences by distilling vision foundation models. In *Advances in Neural Information Processing Systems*, pages 37193–37229, 2023.
- [47] Youquan Liu et al. Multi-space alignments towards universal LiDAR segmentation. In *IEEE/CVF Conference on Computer Vision and Pattern Recognition*, pages 14648–14661, 2024.
- [48] Youquan Liu et al. La La LiDAR: Large-scale layout generation from LiDAR data. In *AAAI Conference on Artificial Intelligence*, pages 7377–7385, 2026.
- [49] Youquan Liu et al. Veila: Panoramic LiDAR generation from a monocular RGB image. In *IEEE International Conference on Robotics and Automation*, 2026.
- [50] Ze Liu, Yutong Lin, Yue Cao, Han Hu, Yixuan Wei, Zheng Zhang, Stephen Lin, and Baining Guo. Swin transformer: Hierarchical vision transformer using shifted windows. In *IEEE/CVF International Conference on Computer Vision*, pages 10012–10022, 2021.

- [51] Zhijian Liu, Xinyu Yang, Haotian Tang, Shang Yang, and Song Han. FlatFormer: Flattened window attention for efficient point cloud transformer. In *IEEE/CVF Conference on Computer Vision and Pattern Recognition*, pages 1200–1211, 2023.
- [52] Tao Lu, Xiang Ding, Haisong Liu, Gangshan Wu, and Limin Wang. Link: Linear kernel for lidar-based 3d perception. In *IEEE/CVF Conference on Computer Vision and Pattern Recognition*, pages 1105–1115, 2023.
- [53] Jiageng Mao, Yujing Xue, Minzhe Niu, Haoyue Bai, Jiashi Feng, Xiaodan Liang, Hang Xu, and Chunjing Xu. Voxel transformer for 3d object detection. In *IEEE/CVF International Conference on Computer Vision*, pages 3164–3173, 2021.
- [54] Lars Mescheder, Michael Oechsle, Michael Niemeyer, Sebastian Nowozin, and Andreas Geiger. Occupancy networks: Learning 3D reconstruction in function space. In *IEEE/CVF Conference on Computer Vision and Pattern Recognition*, pages 4460–4470, 2019.
- [55] Jeong Joon Park, Peter Florence, Julian Straub, Richard Newcombe, and Steven Lovegrove. DeepSDF: Learning continuous signed distance functions for shape representation. In *IEEE/CVF Conference on Computer Vision and Pattern Recognition*, pages 165–174, 2019.
- [56] William Peebles and Saining Xie. Scalable diffusion models with transformers. In *IEEE/CVF International Conference on Computer Vision*, pages 4195–4205, 2023.
- [57] Songyou Peng, Michael Niemeyer, Lars Mescheder, Marc Pollefeys, and Andreas Geiger. Convolutional occupancy networks. In *European Conference on Computer Vision*, pages 523–540. Springer, 2020.
- [58] Christoph B Rist, David Emmerichs, Markus Enzweiler, and Dariu M Gavrilă. Semantic scene completion using local deep implicit functions on lidar data. *IEEE Transactions on Pattern Analysis and Machine Intelligence*, 44(10): 7205–7218, 2021.
- [59] Jason Rock, Tanmay Gupta, Justin Thorsen, JunYoung Gwak, Daeyun Shin, and Derek Hoiem. Completing 3D object shape from one depth image. In *IEEE/CVF Conference on Computer Vision and Pattern Recognition*, pages 2484–2493, 2015.
- [60] Luis Roldao et al. LMSCNet: Lightweight multiscale 3D semantic completion. In *International Conference on 3D Vision*, pages 111–119, 2020.
- [61] Anith Selvakumar and Manasa Bharadwaj. Fake it to make it: Virtual multiviews to enhance monocular indoor semantic scene completion. *arXiv preprint arXiv:2503.05086*, 2025.
- [62] Yiang Shi, Tianheng Cheng, Qian Zhang, Wenyu Liu, and Xinggang Wang. Occupancy as set of points. In *European Conference on Computer Vision*, pages 72–87. Springer, 2024.
- [63] Nathan Silberman, Derek Hoiem, Pushmeet Kohli, and Rob Fergus. Indoor segmentation and support inference from RGB-D images. In *European Conference on Computer Vision*, pages 746–760. Springer, 2012.
- [64] Shuran Song, Fisher Yu, Andy Zeng, Angel X. Chang, Manolis Savva, and Thomas Funkhouser. Semantic scene completion from a single depth image. In *IEEE/CVF Conference on Computer Vision and Pattern Recognition*, pages 1746–1754, 2017.
- [65] Mingxing Tan and Quoc Le. EfficientNet: Rethinking model scaling for convolutional neural networks. In *International Conference on Machine Learning*, pages 6105–6114. PMLR, 2019.
- [66] Ashish Vaswani, Noam Shazeer, Niki Parmar, Jakob Uszkoreit, Llion Jones, Aidan N Gomez, Łukasz Kaiser, and Illia Polosukhin. Attention is all you need. In *Advances in Neural Information Processing Systems*, 2017.
- [67] Peng-Shuai Wang. OctFormer: Octree-based transformers for 3D point clouds. *ACM Transactions on Graphics*, 42(4):1–11, 2023.
- [68] Song Wang, Yu Jiawei, Li Wentong, Liu Wenyu, Liu Xiaolu, Chen Junbo, and Zhu Jianke. Not all voxels are equal: Hardness-aware semantic scene completion with self-distillation. In *IEEE/CVF Conference on Computer Vision and Pattern Recognition*, pages 14792–14801, 2024.
- [69] Song Wang, Jiawei Yu, Wentong Li, Hao Shi, Kailun Yang, Junbo Chen, and Jianke Zhu. Label-efficient semantic scene completion with scribble annotations. In *International Joint Conference on Artificial Intelligence*, pages 1398–1406, 2024.
- [70] Song Wang, Xiaolu Liu, et al. PointLoRA: Low-rank adaptation with token selection for point cloud learning. In *IEEE/CVF Conference on Computer Vision and Pattern Recognition*, pages 6605–6615, 2025.
- [71] Song Wang, Zhongdao Wang, Jiawei Yu, Wentong Li, Bailan Feng, Junbo Chen, and Jianke Zhu. Reliable and calibrated semantic occupancy prediction by hybrid uncertainty learning. In *International Joint Conference on Artificial Intelligence*, pages 1973–1981, 2025.
- [72] Song Wang et al. Forging spatial intelligence: A roadmap of multi-modal data pre-training for autonomous systems. *arXiv preprint arXiv:2512.24385*, 2025.
- [73] Xuzhi Wang, Di Lin, and Liang Wan. FFNet: Frequency fusion network for semantic scene completion. In *AAAI Conference on Artificial Intelligence*, pages 2550–2557, 2022.
- [74] Xuzhi Wang, Xinran Wu, Song Wang, et al. Monocular semantic scene completion via masked recurrent networks. In *IEEE/CVF Conference on International Conference on Computer Vision*, 2025.
- [75] Xuzhi Wang et al. NUC-Net: Non-uniform cylindrical partition network for efficient LiDAR semantic segmentation. *IEEE Transactions on Circuits and Systems for Video Technology*, 35(9):9090–9104, 2025.
- [76] Yi Wei, Linqing Zhao, Wenzhao Zheng, Zheng Zhu, Jie Zhou, and Jiwen Lu. SurroundOCC: Multi-camera 3D occupancy prediction for autonomous driving. In *IEEE/CVF International Conference on Computer Vision*, pages 21729–21740, 2023.
- [77] Xiaoyang Wu, Li Jiang, Peng-Shuai Wang, Zhijian Liu, Xihui Liu, Yu Qiao, Wanli Ouyang, Tong He, and Hengshuang Zhao. Point transformer v3: Simpler faster stronger. In *IEEE/CVF Conference on Computer Vision and Pattern Recognition*, pages 4840–4851, 2024.

- [78] Zhaoyang Xia, Youquan Liu, Xin Li, Xinge Xu, Yuexin Ma, Yikang Li, Yuenan Hou, and Yu Qiao. SCPNet: Semantic scene completion on point cloud. In *IEEE/CVF Conference on Computer Vision and Pattern Recognition*, pages 17642–17651, 2023.
- [79] Shaoyuan Xie et al. Are VLMs ready for autonomous driving? an empirical study from the reliability, data, and metric perspectives. In *IEEE/CVF International Conference on Computer Vision*, pages 6585–6597, 2025.
- [80] Shaoyuan Xie et al. Benchmarking and improving bird’s eye view perception robustness in autonomous driving. *IEEE Transactions on Pattern Analysis and Machine Intelligence*, 47(5):3878–3894, 2025.
- [81] Jingyi Xu et al. Visual foundation models boost cross-modal unsupervised domain adaptation for 3D semantic segmentation. *IEEE Transactions on Intelligent Transportation Systems*, 26(11):20287–20301, 2025.
- [82] Xiang Xu et al. 4D contrastive superflows are dense 3D representation learners. In *European Conference on Computer Vision*, pages 58–80, 2024.
- [83] Xiang Xu et al. FRNet: Frustum-range networks for scalable LiDAR segmentation. *IEEE Transactions on Image Processing*, 34:2173–2186, 2025.
- [84] Xiang Xu et al. Beyond one shot, beyond one perspective: Cross-view and long-horizon distillation for better LiDAR representations. In *IEEE/CVF International Conference on Computer Vision*, pages 25506–25518, 2025.
- [85] Xiang Xu et al. LiMoE: Mixture of LiDAR representation learners from automotive scenes. In *IEEE/CVF Conference on Computer Vision and Pattern Recognition*, pages 27368–27379, 2025.
- [86] Xiang Xu et al. Enhanced spatiotemporal consistency for image-to-LiDAR data pretraining. *IEEE Transactions on Pattern Analysis and Machine Intelligence*, 48(3):3819–3834, 2026.
- [87] Kai Yan, Fujan Luan, Miloš Hašan, Thibault Groueix, Valentin Deschaintre, and Shuang Zhao. Psdr-room: Single photo to scene using differentiable rendering. In *SIGGRAPH Asia*, pages 1–11, 2023.
- [88] Xu Yan, Jiantao Gao, Jie Li, Ruimao Zhang, Zhen Li, Rui Huang, and Shuguang Cui. Sparse single sweep LiDAR point cloud segmentation via learning contextual shape priors from scene completion. In *AAAI Conference on Artificial Intelligence*, pages 3101–3109, 2021.
- [89] Lihe Yang, Bingyi Kang, Zilong Huang, Xiaogang Xu, Jiashi Feng, and Hengshuang Zhao. Depth anything: Unleashing the power of large-scale unlabeled data. In *IEEE/CVF Conference on Computer Vision and Pattern Recognition*, pages 10371–10381, 2024.
- [90] Jiawei Yao, Chuming Li, Keqiang Sun, Yingjie Cai, Hao Li, Wanli Ouyang, and Hongsheng Li. NDC-Scene: Boost monocular 3D semantic scene completion in normalized device coordinates space. In *IEEE/CVF International Conference on Computer Vision*, pages 9421–9431, 2023.
- [91] Hongxiao Yu, Yuqi Wang, Yuntao Chen, and Zhaoxiang Zhang. Monocular occupancy prediction for scalable indoor scenes. In *European Conference on Computer Vision*, pages 38–54, 2024.
- [92] Cheng Zhang, Zhaopeng Cui, Yinda Zhang, Bing Zeng, Marc Pollefeys, and Shuaicheng Liu. Holistic 3D scene understanding from a single image with implicit representation. In *IEEE/CVF Conference on Computer Vision and Pattern Recognition*, pages 8833–8842, 2021.
- [93] Yunpeng Zhang, Zheng Zhu, and Dalong Du. OccFormer: Dual-path transformer for vision-based 3D semantic occupancy prediction. In *IEEE/CVF International Conference on Computer Vision*, pages 9433–9443, 2023.
- [94] Yiyuan Zhang, Xiaohan Ding, and Xiangyu Yue. Scaling up your kernels: Large kernel design in convnets towards universal representations. *IEEE Transactions on Pattern Analysis and Machine Intelligence*, 2025.
- [95] Linqing Zhao, Xiuwei Xu, Ziwei Wang, Yunpeng Zhang, Borui Zhang, Wenzhao Zheng, Dalong Du, Jie Zhou, and Jiwen Lu. LowRankOcc: tensor decomposition and low-rank recovery for vision-based 3D semantic occupancy prediction. In *IEEE/CVF Conference on Computer Vision and Pattern Recognition*, pages 9806–9815, 2024.
- [96] Qingcheng Zhao, Xiang Zhang, Haiyang Xu, Zeyuan Chen, Jianwen Xie, Yuan Gao, and Zhuowen Tu. DEPR: Depth guided single-view scene reconstruction with instance-level diffusion. *arXiv preprint arXiv:2507.22825*, 2025.
- [97] Jilai Zheng, Pin Tang, Zhongdao Wang, Guoqing Wang, Xiangxuan Ren, Bailan Feng, and Chao Ma. Veon: Vocabulary-enhanced occupancy prediction. In *European Conference on Computer Vision*, pages 92–108. Springer, 2024.
- [98] Wenzhao Zheng, Weiliang Chen, Yuanhui Huang, Borui Zhang, Yueqi Duan, and Jiwen Lu. OccWorld: Learning a 3D occupancy world model for autonomous driving. In *European conference on computer vision*, pages 55–72. Springer, 2024.
- [99] Yupeng Zheng, Xiang Li, Pengfei Li, Yuhang Zheng, Bu Jin, Chengliang Zhong, Xiaoxiao Long, Hao Zhao, and Qichao Zhang. MonoOCC: Digging into monocular semantic occupancy prediction. In *IEEE International Conference on Robotics and Automation*, pages 18398–18405, 2024.
- [100] Junsheng Zhou, Yu-Shen Liu, and Zhizhong Han. Zero-shot scene reconstruction from single images with deep prior assembly. *Advances in Neural Information Processing Systems*, 37:39104–39127, 2024.
- [101] Benjin Zhu, Zhe Wang, and Hongsheng Li. nuCraft: Crafting high resolution 3D semantic occupancy for unified 3D scene understanding. In *European Conference on Computer Vision*, pages 125–141. Springer, 2024.
- [102] Dekai Zhu, Yixuan Hu, Youquan Liu, et al. SPIRAL: Semantic-aware progressive LiDAR scene generation. In *Advances in Neural Information Processing Systems*, 2025.